



Research on drought evolution using multi-temporal remote sensing on Google Earth Engine platform

Thanh Hoa Pham Thi¹, Thinh Nguyen Van²

¹Hanoi University of Mining and Geology, Vietnam

E-mail: phamthithanhhoa@humg.edu.vn

²University of Transport Technology, Vietnam

Abstract The advantages of Google Earth Engine (GEE) platform include the integration of different satellite imagery at different resolutions, temporal and spatial scales with high-speed parallel processing capabilities and machine learning algorithms. Therefore, it has been considered an effective tool for monitoring severe drought. Our objectives are to investigate drought evolution and spatiotemporal variations from 2015 to 2020 based on a remote-sensing index, namely, the Water Supplying Vegetation Index (WSVI) which was extracted from Landsat 8 OLI/TIRS on GEE. The study area is Binh Dinh province which is indicated as a subject of prolonged droughts during dry seasons. Results showed that the severe and moderate drought areas were concentrated mainly in some districts such as Hoai Nhon, Phu My, An Nhon, Tay Son, Tuy Phuoc and Quy Nhon districts, corresponding to low WSVI values. To validate our results, the drought map in 2015 in this study was chosen to compare with the map established by using Modis imagery in Binh Dinh in the same year. Although the different resolutions between two images, we identified similar drought areas on two maps. In general, the results also reflect the reliability of the method and the advantages of GEE in monitoring drought in remote and small areas.

Keywords Drought, WSVI, Google Earth Engine, Binh Dinh

1. Introduction

A drought is an extended period of unusually dry weather when an area or region experiences below-normal precipitation [1]. It is one of the most serious disasters in the world because it impacts the environment, ecosystems, economy and society. Therefore, research on drought monitoring techniques and assessment methods has become an important problem for the government, the authority and all people. Many researchers used traditional meteorological monitoring methods [2-3]. However, this method is still limited in comprehensive drought monitoring for application on a large scale and in an area with few monitoring stations. In addition, the integration of free remote sensing imagery into Google Earth Engine – a platform based on cloud computing – has brought the trend in studying agriculture, vegetation mapping and monitoring, natural disasters and earth sciences [4]. Google Earth Engine (GEE) has the advantage of being macroscopic, rapid and providing continuous data in time and space with high-speed parallel processing capabilities and machine learning algorithms [5]. Many scientists recognized the potential of using GEE for monitoring drought. Aksoy et al., [6] and [7] analyzed the temporal distribution of drought conditions within years using different drought indices produced from MODIS satellite data in the GEE platform. These results showed that remote sensing imagery provided useful spatial information for assessing drought conditions from the regional level to the



country level. Besides, the processing on GEE allows for easy analysis and visualization. Simultaneously it helps explore spatial and temporal variations in information and drought conditions for any location in the world. Therefore, the main objective of this study is to explore the efficiency of using the Google Earth Engine (GEE) platform for assessing drought conditions by multi-temporal satellite imagery such as Landsat 8 OLI/TIRS. Compared with MODIS, the bands in Landsat 8 have a higher spatial resolution of 100 m (thermal bands) /30 m (multi-spectral bands) and can be used to retrieve the drought index at a finer scale. The study investigated drought evolution and spatiotemporal variations from 2015 to 2020 based on a remote-sensing index, namely, the Water Supplying Vegetation Index (WSVI). It combines two indices components as NDVI and LST which provides a strong correlation and gives useful information to identify drought [8]. The study area is Binh Dinh province which is indicated as a subject of prolonged droughts during dry seasons.

2. Materials

2.1. Study Area



Figure 1: The study area

Binh Dinh is a province of Vietnam. It is located in Vietnam's South Central Coast region. Most districts of Binh Dinh have a topography that is a mix of mountains or hills and lowlands (*Wikipedia*). Binh Dinh is in the tropical region with high humidity and prevalent southerly and northerly winds during the dry and wet seasons respectively. The dry season is from January to August and the wet season is from September to December. During the dry season in Binh Dinh, the rainfall is very little, only 20-25%, the temperature is high, the evaporation is large and prolonged. In addition, the terrain is steep, the river basins are short, so the rivers cannot store water. Therefore, long droughts are often observed during the dry season. The prolonged drought has caused serious water shortages for many people in Binh Dinh province. Besides, the impacts of drought tend to cause a lot of environmental, economic and social damage. Drought can also cause long-term public health problems.



It can be mentioned that the prolonged hot weather in 2016 and 2019 caused Binh Dinh people to face the most severe drought in the last 15 years. Prolonged drought in recent months has caused serious water shortages for more than 4000 households in many localities in Binh Dinh. According to the province's Agriculture and Rural Development Department in 2016, more than 3,400ha of crops face water shortages and about 200ha of summer-autumn rice has died of the drought. Quy Nhon City and the districts of Phu My, Hoai Nhon, Hoai An, Tay Son and Tuy Phuoc have been hit the hardest by drought as the affected cultivation areas ranged from 163ha to nearly 700ha: Quy Nhon (697 ha); Phu My district (499 ha); Hoai Nhon (344 ha); Hoai An (340 ha); Tay Son (237 ha); Tuy Phuoc (163 ha).

2.2. Data resources

For this study, Landsat 8 OLI and TIRS in Google Earth Engine were used for the analysis. This data can be looked up at the GEE catalog via the website <https://developers.google.com/earth-engine/datasets/catalog/landsat>. The spatial resolution of thermal infrared bands is 100 meters but has been resampled to 30 m, similar to multispectral bands. We chose the Landsat 8 image scenes which covered the entire study area during the dry season from 2015 to 2020. In which, TOA (top-of-atmosphere reflectance) and SR (surface reflectance) data are appropriate for calculating the index in this research. TOA data were converted from raw digital numbers values using the calibration coefficients from the image metadata [9]. The SR data were generated using the Land Surface Reflectance Code (LaSRC) algorithm [10].

3. Methodology

In this study, for drought analysis, using data from the Google Earth Engine platform, the drought index WSVI (Water Supplying Vegetation Index) was calculated from 2015 to 2020. The methodology for calculations is described below in detail.

$$WSVI = \frac{NDVI}{LST} \quad (1) [11]$$

Whereas,

NDVI (Normalized Difference Vegetation Index) is used to quantify vegetation greenness and is useful in understanding vegetation density and assessing changes in plant health. This index defines values from -1.0 to 1.0, the higher value of NDVI refers to healthy and dense vegetation, where negative values are mainly formed from clouds, water and snow, and values close to zero are primarily formed from rocks and bare soil. NDVI is calculated as a ratio between the red (R) and near infrared (NIR) values with the formula:

$$NDVI = \frac{NIR-RED}{NIR+RED} \quad (2) [12]$$

LST (Land Surface Temperature) is calculated based on the brightness temperature results taking into account the influence of land surface emissivity [13]:

$$LST = \frac{T_B}{1 + \left(\frac{\lambda \cdot T_B}{\rho}\right) \cdot \ln LSE} \quad (3)$$

T_B is Top of Atmosphere Brightness Temperature (TOA temperature) for TIR bands of Landsat which are fully available and ready to use in GEE;

$\rho = 14380$, $\rho = h \cdot c / s$ with h is Plank's constant ($6,626 \cdot 10^{-34}$ Js), s is Boltzmann's constant ($1,38 \cdot 10^{-23}$ J/K), c is velocity of light ($3 \cdot 10^8$ m/s);

λ is the value of the central wavelength of thermal infrared band

LSE is Land Surface Emissivity, was computed based on P_v (Proportion of Vegetation) (Sobrino et al., 2004), with a value of 0.004 being the standard deviation of 49 soil spectra, and 0.986 is considered as the average of soil emissivity and vegetation emissivity.

$$LSE = 0.004P_v + 0.986 \quad (4)$$

With

$$P_v = \left(\frac{NDVI - NDVI_{min}}{NDVI_{max} - NDVI_{min}} \right)^2 \quad (5)$$



The WSVI index is the one of indices developed to combine NDVI and LST data to detect drought conditions [14]. It is based on the fact that, in drought conditions, NDVI values will drop below normal while temperatures are observed to rise above normal.

In this study, JavaScript programming algorithms on GEE Code Editor were used to add Landsat 8 OLI/TIR image to the platform and perform steps including processing, analyzing, displaying and exporting results.

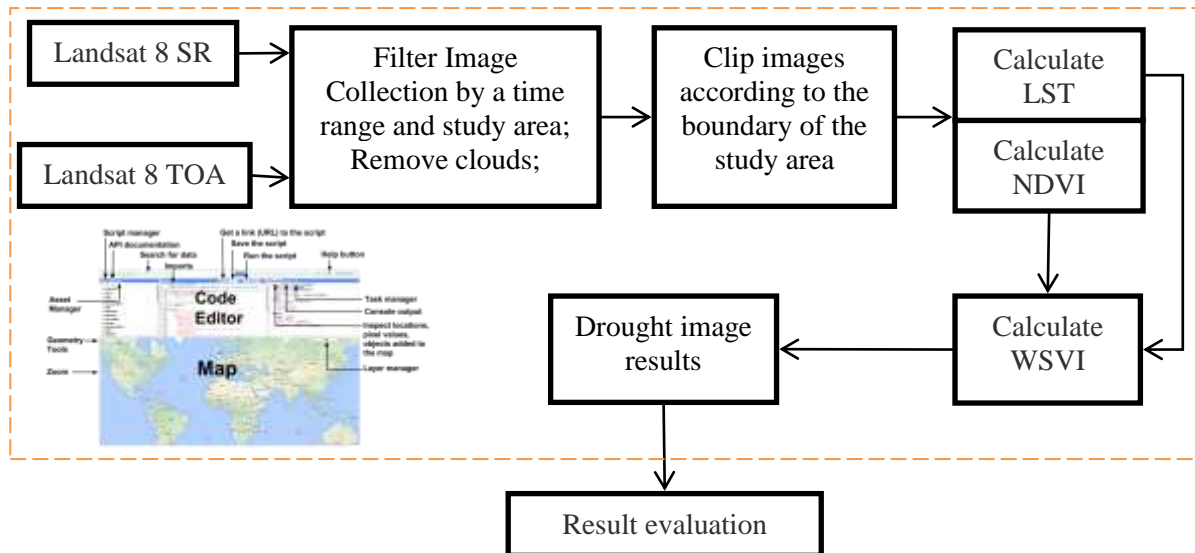
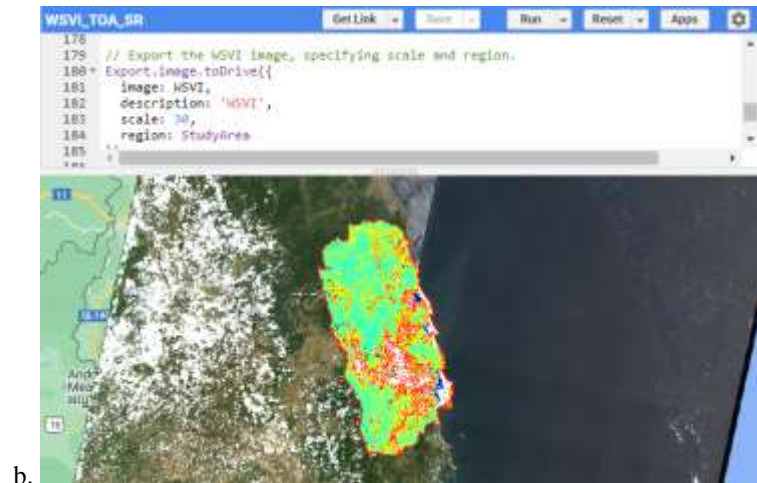


Figure 2: Workflow of research

4. Results and Discussion

With the GEE platform, we used the algorithms/ functions to write and execute scripts for processing in figure 2 and calculating the indices: Normalized Difference Vegetation Index (NDVI), Land Surface Temperature (LST), WSVI (Water Supplying Vegetation Index).





b.

Figure 3: Results in GEE

a. Collection of Landsat 8 images of the study area

b. Script and drought result in GEE

4.1. The spatial distributions of NDVI and LST

Figure 4 shows the spatial distributions of NDVI and LST in Binh Dinh province in 2015 [15]. The higher values of NDVI (the yellow and red areas) indicate the information of health dense vegetation corresponding to the forest or the agricultural area. While lower values represented stressed vegetation, the negative values correspond to areas with water surfaces or high moisture content, respectively. With the LST map in the dry season in 2015, nearly two-thirds of the study area has a surface temperature higher than 25°C (orange and red area), in which the highest temperature is above 42°C.

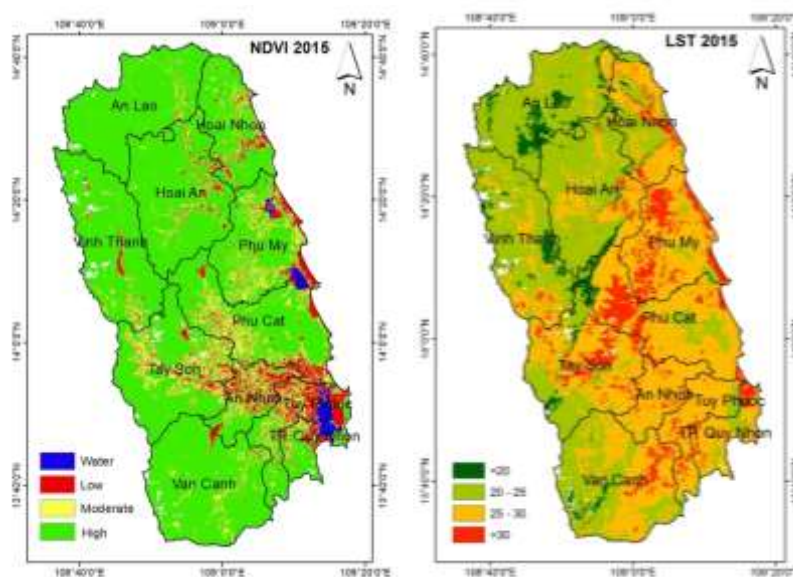


Figure 4: The spatial distributions of NDVI and LST in Binh Dinh in 2015

In comparison between NDVI and LST images, in areas where high LST values were observed, the NDVI diminished due to the variation in vegetation state. Spatially, the distributions of low and medium values of NDVI and high values of LST (shown in red and yellow in two images) are mostly concentrated in the coastal area, near the center and the south of Binh Dinh province. It is evaluated that the land surface temperatures are higher and increase more markedly in areas of sparse vegetation cover. Conversely, dense



vegetation cover absorbs the land surface temperature. In the following years, these results are also similar. Overall, they are also considered tools for monitoring periods of drought, NDVI at a given pixel will typically be relatively low, whereas LST is expected to be relatively high because of vegetation deterioration.

4.2. Spatial variation of drought in Binh Dinh province

When drought occurs, the value range of WSVI is between -4,2 and +4,2, the smaller value of the index means the less vegetation water supply and the more severe drought. In the same way, a greater value means a less severe drought [14]. The results of the WSVI index maps of Binh Dinh province in a 6-year period (2015-2020) are shown in Figure 5.

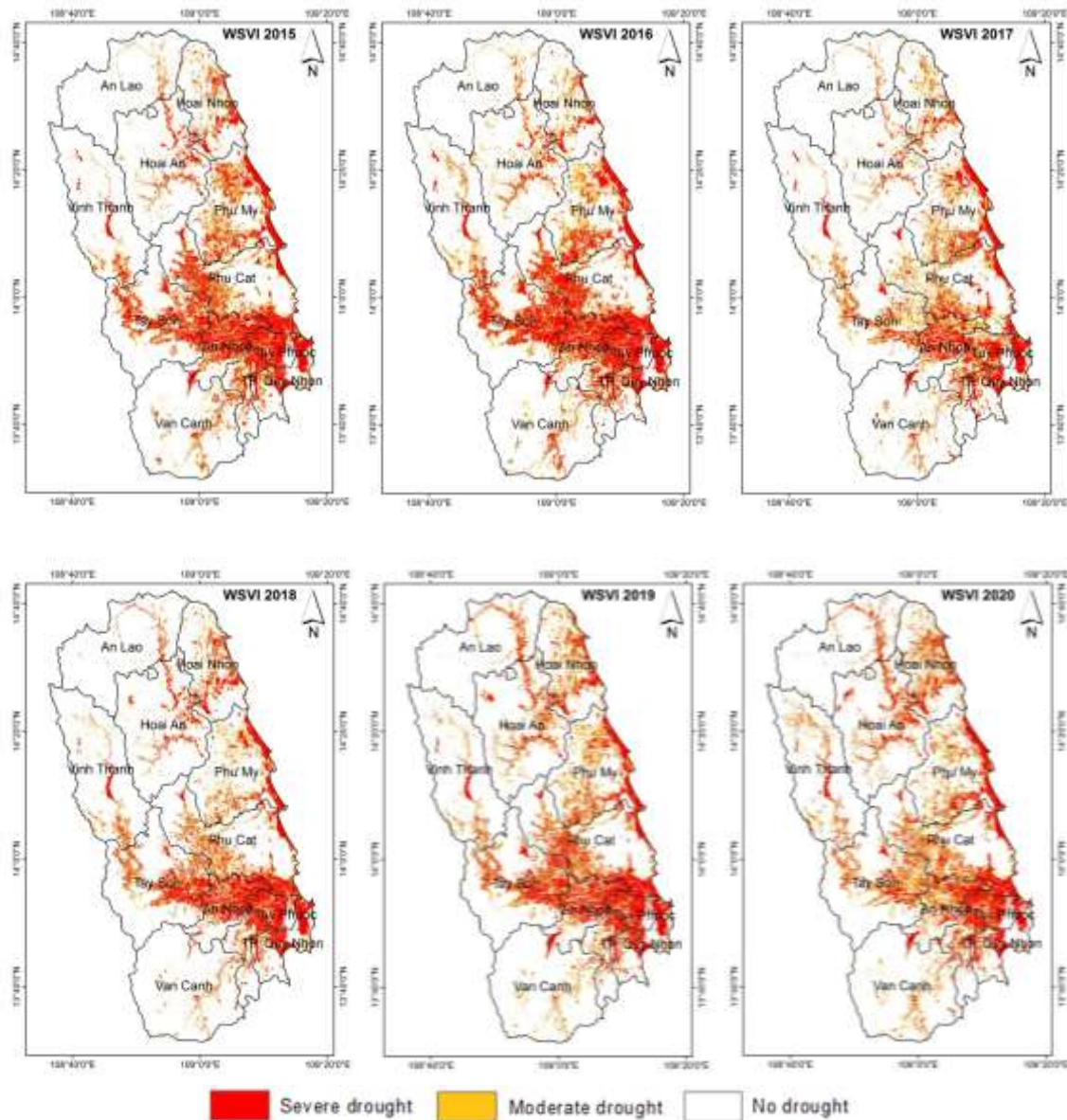


Figure 5: Drought maps with WSVI index in Binh Dinh from 2015 to 2020

The results of the study showed that in the period from 2015 to 2020, the drought situation occurred almost across the entire territory of Binh Dinh province, of varying intensity. Drought impacts were especially serious in the Eastern coastal area or the area near the center of Binh Dinh province, including Hoai Nhon, Phu My, An



Nhon, Tay Son, Tuy Phuoc and Quy Nhon districts. The severe and moderate drought (red and orange on the map) tends to increase during the 2015–2016 and 2017 - 2018 dry seasons. In contrast, from 2016 to 2017 and from 2018 to 2020, it tends to decrease but slowly. Considering this period, the drought area accounted for the highest proportion in 2016 with 40.1% and 2019 with 39% and they considered more severe drought years than other years; On the contrary, in 2020 the drought area is lower than other years. At the same time, the results also show an important role of vegetative cover in reducing drought risk, the areas which were covered by forest or strong vegetation, are less affected by drought. These results are suitable for the drought situation which was recorded in the climate assessment report of Binh Dinh province [15].

The results of drought distribution with WSVI index were compared with the drought map of Binh Dinh province in 2015 using MODIS image. In terms of space, the overlap of maps shows similarly in the distribution of drought areas in the study area. Quantitative statistics show that the drought area difference is 12.6% with the WSVI index in 2015. This difference is because the reference term map established from Modis image data with a lower resolution than the Landsat 8 image used in this study. However, in general, the obtained results also reflect the reliability of the method using the Google Earth Engine platform in drought research.

5. Conclusion

This study applied JavaScript programming on the Google Earth Engine platform to quickly create the preliminary results about the spatial distribution of drought with the case study in Binh Dinh province from 2015 to 2020, using Water Supplying Vegetation Index (WSVI) from Landsat 8 images. GEE and its tools allow users to easily analyze data for any area over the world without downloading and processing a large amount of imagery data on a personal computer or laptop. The programming instead of calculations by image processing software has brought high efficiency, allowing to determine the intensity, severity and spatial extent of drought. Finally, it is necessary to combine the meteorology parameters (rainfall, humidity...), different types of satellite imagery in GEE and other methods to create a comprehensive drought monitoring model in the future.

References

- [1]. Panagoulia, D. (1998). *Definitions and effects of droughts*. In Proceedings of the Conference on Mediterranean Water Policy: Building on Existing Experience, Mediterranean Water Network, Valencia, Spain.
- [2]. McKee, T. B., Doesken, N. J., & Kleist, J. R. (1993). *The relationship of drought frequency and duration to time scales*. In Proceedings of the Eighth Conference on Applied Climatology, American Meteorological Society.
- [3]. Palmer, W. C. (1965). Meteorological Drought. *Research Paper No. 45, US Weather Bureau, Washington, DC*.
- [4]. Mutanga, O., & Kumar, L. (2019). Google Earth Engine Applications. *Remote Sensing, 11*, 591. doi: 10.3390/rs11050591
- [5]. Gorelick, N., Hancher, M., Dixon, M., Ilyushchenko, S., Thau, D., & Moore, R. (2017). Google Earth Engine: Planetary-scale geospatial analysis for everyone. *Remote Sensing of Environment, 202*, 18-27. doi: <https://doi.org/10.1016/j.rse.2017.06.031>
- [6]. Aksoy, S., Gorucu, O., & Sertel, E. (2019). *Drought Monitoring using MODIS derived indices and Google Earth Engine Platform*. In 2019 8th International Conference on Agro-Geoinformatics (Agro-Geoinformatics).
- [7]. Khan, R., Gilani, H., Iqbal, N., & Shahid, I. (2019). Satellite-based (2000–2015) drought hazard assessment with indices, mapping, and monitoring of Potohar plateau, Punjab, Pakistan. *Environmental Earth Sciences, 79*(1), 23. doi: 10.1007/s12665-019-8751-9
- [8]. Sruthi, S., & Aslam, M. A. M. (2015). Agricultural Drought Analysis Using the NDVI and Land Surface Temperature Data; a Case Study of Raichur District. *Aquatic Procedia, 4*, 1258-1264. doi: <https://doi.org/10.1016/j.aapro.2015.02.164>



- [9]. Chander, G., Markham, B. L., & Helder, D. L. (2009). Summary of current radiometric calibration coefficients for Landsat MSS, TM, ETM+, and EO-1 ALI sensors. *Remote Sensing of Environment*, 113(5), 893-903. doi: <https://doi.org/10.1016/j.rse.2009.01.007>.
- [10]. Vermote, E., Justice, C., Claverie, M., & Franch, B. (2016). Preliminary analysis of the performance of the Landsat 8/OLI land surface reflectance product. *Remote sensing of environment, Volume 185*(Iss 2), 46-56. doi: 10.1016/j.rse.2016.04.008
- [11]. Xiao, X., Longhua, H., Salas, W., Li, C., Moore, B., Zhao, R., . . . Boles, S. (2002). Quantitative relationships between field-measured leaf area index and vegetation index derived from VEGETATION images for paddy rice fields. *International Journal of Remote Sensing - INT J REMOTE SENS*, 23, 3595-3604. doi: 10.1080/01431160110115799
- [12]. Tucker, C. J. (1979). Red and photographic infrared linear combinations for monitoring vegetation. *Remote Sensing of Environment*, 8(2), 127-150. doi: [https://doi.org/10.1016/0034-4257\(79\)90013-0](https://doi.org/10.1016/0034-4257(79)90013-0)
- [13]. Weng, Q., Lu, D., & Schubring, J. (2004). Estimation of land surface temperature–vegetation abundance relationship for urban heat island studies. *Remote Sensing of Environment*, 89(4), 467-483. doi: <https://doi.org/10.1016/j.rse.2003.11.005>
- [14]. Alshaikh, A. Y. (2015). Space applications for drought assessment in Wadi-Dama (West Tabouk), KSA. *The Egyptian Journal of Remote Sensing and Space Science*, 18(1, Supplement 1), S43-S53. doi: <https://doi.org/10.1016/j.ejrs.2015.07.001>
- [15]. Binh Dinh Department of Natural Resources and Environment. (2019). *The climate assessment report of Binh Dinh province*

